# Boundary Element Methods for the Analysis of Crack Growth in the Presence of Residual Stress Fields

*V.M.A. Leitao, M.H. Aliabadi, D.P. Rooke, and R. Cook*

*(Submitted 15 August 1997; in revised form 13 January 1998)*

**Two boundary element methods of simulating crack growth in the presence of residual stress fields are presented, and the results are compared to experimental measurements. The first method utilizes linear elastic fracture mechanics (LEFM) and superimposes the solutions due to the applied load and the residual stress field. In this method, the residual stress fields are obtained from an elastoplastic BEM analysis, and numerical weight functions are used to obtain the stress intensity factors due to the fatigue loading. The second method presented is an elastoplastic fracture mechanics (EPFM) approach for crack growth simulation. A nonlinear J-integral is used in the fatigue life calculations. The methods are shown to agree well with experimental measurements of crack growth in prestressed open hole specimens. Results are also presented for the case where the prestress is applied to specimens that have been precracked.**

**Keywords** BEM, cold expansion, fracture mechanics, nonlinear analysis

## 1. Introduction

Surface treatment techniques are increasingly being used by manufacturers to enhance the fatigue performance of critical parts. These techniques introduce residual stress fields into the part. The residual stress fields affect the fatigue life of the components; compressive stresses generally prolong fatigue life by reducing crack growth rates and possibly by delaying crack initiation, whereas tensile stresses generally reduce fatigue life. The ability to predict the effect of the surface treatment on the fatigue life of the components is important because the rate of growth of a crack will determine when the component must be repaired or replaced.

Considerable interest in the influence of residual stresses on the crack growth occurred in the 1970s, particularly in aircraft industries. Among the first published studies are those of Potter and Grandt (Ref 1) in 1975 when the superposition procedure was first proposed and Rich and Impellizzeri (Ref 2) in 1976 where some correlations between analytical and experimental results were shown. Later, Chang (Ref 3) presented additional correlations and a procedure that uses approximate analytical stress solutions for both the residual and applied stresses. At approximately the same time, Hsu and Aberson (Ref 4) used a Green's function approach to determine the stress intensity factors due to the residual stress fields. This work was extended to interface-fit fastener holes by the same authors and Rudd (Ref 5). Armen, Levy, and Eidinoff (Ref 6) used weight functions for a crack at a hole in a finite width plate to calculate the residual stress intensity factors from residual stress states determined from a nonlinear finite element method (FEM). Cook et al. (Ref 7) presented and compared a numerical study (by using a nonlinear FEM formulation combined with Green's functions) and an experimental investigation of crack growth rates for components subjected to prestress. Other authors, for example Mann and Sparrow (Ref 8), Buxbaum and Huth (Ref 9), Heller et al. (Ref 10), Heller and Carey (Ref 11), and Clarck (Ref 12) have developed the subject. More recent research is found in Aliabadi and Brebbia (Ref 13) and Aliabadi and Terranova (Ref 14).

Two boundary element methods (BEM) are used to study the fatigue crack growth in the presence of residual stress fields. The first method utilizes an elastoplastic BEM to evaluate the residual stresses due to uniform prestress applied at the ends of a component containing a central hole (Ref 15). The linear elastic weight function method is then used to obtain the stress intensity factor due to the fatigue load as well as the residual stress fields. Crack growth rates are computed and compared with experimental measurements. The second technique uses a newly developed dual (BEM) formulation for elastoplastic simulation of fatigue crack growth (Ref 16). In this method, a nonlinear J-integral is used to evaluate the equivalent stress intensity factors. Results are obtained for both an initially smooth specimen and a precracked specimen.

## 2. Linear Elastic Fracture Mechanics (LEFM) Approach

In the linear elastic fracture mechanics (LEFM) approach, it is assumed that the residual stresses formed by the prestress of the uncracked hole are not affected by the presence and growth of a fatigue crack. The residual stress distribution can be considered as a mean stress contribution, which affects the stress intensity factor ratio $R$, but not the range $\Delta K$, as shown below. In the LEFM, the principle of superposition is valid, and in the presence of residual stresses, the parameter $K$ can be expressed as:

$$K = K_{\text{total}} = K_{\text{applied load}} + K_{\text{residual stresses}} \quad \text{(Eq 1)}$$

**V.M.A. Leitao,** Technical University of Lisbon, Lisbon, Portugal; **M.H. Aliabadi,** Department of Engineering, QMW, University of London, London E1 4NS, UK; **D.P. Rooke** and **R. Cook,** Defence Research Agency, Farnborough, UK.

For the minimum and maximum applied stress levels Eq 1 can be expressed as:

$$K^{\max} = K_{\text{tot}}^{\max} = K_{\text{app}}^{\max} + K_{\text{res}} \quad \text{(Eq 2)}$$

and

$$K^{\min} = K_{\text{tot}}^{\min} = K_{\text{app}}^{\min} + K_{\text{res}} \quad \text{(Eq 3)}$$

so it follows from the above equations that

$$\Delta K = K_{\text{app}}^{\max} - K_{\text{app}}^{\min} \quad \text{(Eq 4)}$$

which is independent of $K_{\text{res}}$. The stress intensity ratio, $R$, is given by:

$$R = R_{\text{tot}} = \frac{K_{\text{tot}}^{\min}}{K_{\text{tot}}^{\max}} = \frac{K_{\text{app}}^{\min} + K_{\text{res}}}{K_{\text{app}}^{\max} + K_{\text{res}}} \quad \text{(Eq 5)}$$

In contrast to $\Delta K$, the effect of Kres, particularly when it is large and negative, is important in determining $R$.

### *2.1 Stress Intensity Factor Calculations*

Weight functions (WF), are the displacement boundary fields in an elastic body created by the application of a pair of opposing unit forces acting on the crack faces near to the crack tip. The main aspect of the weight functions is that they satisfy the equations of linear elasticity, but present a singularity at the crack tip which normally would not be admissible as a physical field. Due to this characteristic, Bueckner named them " fundamental fields." Applying Betti's reciprocity theorem, the stress intensity factor for a given state can be obtained from the knowledge of Bueckner's fundamental fields and the boundary tractions for that given state.

Aliabadi and Rooke (Ref 17) showed that the stress intensity factors for modes I and II can be obtained from a generalized integral expression:

$$K_N^{(1)} = \frac{E'}{4\sqrt{2\pi B^N}} \int_\Gamma \mathbf{t}^{(1)} \cdot \mathbf{u}_N^{(2)}\, d\Gamma \quad N = \text{I, II} \quad \text{(Eq 6)}$$

where $\Gamma$ is the boundary on which the known surface tractions $\mathbf{t}^{(1)}$ are applied and $B_N$ is the strength of the singular fields (Ref 18). In this equation, $E' = E/(1 - \nu^2)$ for plane strain and $E' = E$ for plane stress. The term $\mathbf{u}_N^{(2)}$ represents the displacement field on the boundary $\Gamma$, which results from the singular field of strength $B_N$ at the crack tip.

As stated, one of the consequences of the application of LEFM is that the principle of superposition is valid. Hence, the loads acting on a body can be studied independently, and the separate effects can be added together. The end result is the same as if all the loads had been jointly applied. The calculation of stress intensity factors for a cracked body subjected to both residual stress on the crack faces and a remote load is described in the following sections.

**Stress Intensity Factors for the Remote Load.** The stress intensity factor for the applied load can be obtained using Eq 6:

$$K_{\text{I}_{\text{app}}}^{(1)} = \frac{E'}{4\sqrt{2\pi B^{\text{I}}}} \int_{\Gamma_{\text{app}}} \sigma_{\text{app}} u_{2\text{I}}^{(2)} d\Gamma \quad \text{(Eq 7)}$$

where $\Gamma_{\text{app}}$ represents the boundary on which the load, $\sigma_{\text{app}}$, is applied and $u_{2\text{I}}^{(2)}$ represents the component of $u_{\text{I}}^{(2)}$ in the direction of the load. In this case, the integrand is regular, and a simple Gauss integration scheme can be used (Ref 15).

**Stress Intensity Factors for Loading on the Crack Faces.** Residual stresses develop around stress concentrations that are the regions where it is most likely a crack will initiate. Prior to the initiation of a crack, residual stresses may be present along the crack path. The determination of the stress intensity factor due to these residual stresses on the crack faces present more difficulties than for remote loading. Because these tractions have to be integrated by a weight function that is singular at the crack tip, special integration techniques must be used. The stress intensity factor is given by:

$$K_{\text{I}_{\text{res}}}^{(1)} = \frac{E'}{4\sqrt{2\pi B_{\text{I}}}} \int_{\Gamma_{\text{res}}} \sigma_{\text{res}} u_{2\text{I}}^{(2)}\, d\Gamma \quad \text{(Eq 8)}$$

where $\Gamma_{\text{res}}$ represents that part of the crack faces which are within the region of the residual stress fields, $\sigma_{\text{res}}$. Because of the singular behavior of the crack face weight function, $O(\frac{1}{\sqrt{r}})$, where $r$ is the distance to the crack tip, a Gauss Chebyshev rule that takes into account this type of singularity was used. This procedure is necessary if accurate values of the integral are to be obtained.

**Numerical Weight Functions.** The weight functions are obtained numerically using BEM rather than analytically because numerical weight functions can be obtained for any geometry, whereas analytical weight functions are restricted to simple geometries. However, there are some numerical difficulties due to the singularity in the fundamental fields. A formulation that subtracts the singular part of the stress fields, known as the subtraction of fundamental fields techniques (SFF) was used in this work. See Aliabadi, Rooke, and Cartwright (Ref 20).

## 3. Elastoplastic Fracture Mechanics (EPFM)

The formulation proposed by Leitao, Aliabadi, and Rooke (Ref 21), is briefly described here. In this formulation, the traction boundary integral equation is used together with the displacement boundary integral equation in a way that overcomes the need for subregions in general mixed-mode elastoplastic fracture mechanics (EPFM) problems. The von Mises yield criterion and the elastoplastic relationship, described by Mendelson (Ref 22), between equivalent total strains and increments

of equivalent plastic strain due to a given load increment were adopted.

Assuming that the material is homogeneous, the boundary integral representation of the displacement components $\dot{u}_i$ (where the dot denotes dependence on the load history) for points at the boundary can be expressed as follows:

$$c_{ij}\dot{u}_j(\mathbf{x}') + \int_\Gamma T_{ij}(\mathbf{x}', \mathbf{x})\dot{u}_j(\mathbf{x})d\Gamma(\mathbf{x}) = \int_\Gamma U_{ij}(\mathbf{x}', \mathbf{x})\dot{t}_j(\mathbf{x})d\Gamma(\mathbf{x}) + \int_\Omega \sigma_{jki}(\mathbf{x}', \mathbf{x})\dot{\varepsilon}^p_{jk}(\mathbf{x})d\Omega(\mathbf{x}) \quad \text{(Eq 9)}$$

where $\mathbf{x}'$ and $\mathbf{x}$ are the source point and the field points, respectively; $\dot{t}_j$ are the boundary tractions; $\Gamma$ and $\Omega$ are the boundary and the domain of the body, respectively; $U_{ij}$, $T_{ij}$, and $\sigma_{jki}$ are known as the Kelvin fundamental solutions and represent the generalized displacements, tractions, and stresses in an infinite, elastic and homogeneous body subjected to unit forces. See Aliabadi and Rooke (Ref 17). The plastic strains are represented by the plastic strain tensor $\dot{\varepsilon}^p_{jk}$, and $c_{ij}$ is a constant that depends on the geometry at the collocation point.

The second equation required on one of the crack surfaces for the implementation of the dual boundary element method is the traction boundary integral equation. This can be obtained by the differentiation of the displacement boundary integral equation given in Eq 9 followed by the application of Hooke's law and the definition of tractions:

$$\dot{t}_i = \dot{\sigma}_{ij}n_j \quad \text{(Eq 10)}$$

where $n_j$ denotes the components of the outward normal vector to the boundary. This results in:

$$\frac{1}{2}\dot{t}_j(\mathbf{x}') + n_i(\mathbf{x}')\int_\Gamma T_{ijk}(\mathbf{x}', \mathbf{x})\dot{u}_k(\mathbf{x})d\Gamma(\mathbf{x}) = n_i(\mathbf{x}')\int_\Gamma U_{ijk}(\mathbf{x}', \mathbf{x})\dot{t}_k(\mathbf{x})d\Gamma(\mathbf{x}) + n_i(\mathbf{x}')\left[\int_\Omega \sigma_{ijkl}(\mathbf{x}', \mathbf{x})\dot{\varepsilon}^p_{kl}(\mathbf{x})d\Omega(\mathbf{x}) + \frac{1}{2}f_{ij}(\dot{\varepsilon}^p_{kl})\right] \quad \text{(Eq 11)}$$

where $T_{ijk}$ and $U_{ijk}$ contain derivatives of $T_{ij}$ and $U_{ij}$, respectively, and the independent term $f_{ij}$ results from the differentiation of the domain integral in Eq 11.

The stress at internal points are obtained from the following equations:

$$\dot{\sigma}_{ij}(\mathbf{x}') = \int_\Gamma U_{ijk}(\mathbf{x}', \mathbf{x})\dot{t}_k(\mathbf{x})d\Gamma(\mathbf{x}) - \int_\Gamma T_{ijk}(\mathbf{x}', \mathbf{x})\dot{u}_k(\mathbf{x})d\Gamma(\mathbf{x}) + n_i(\mathbf{x}')\left[\int_\Omega \sigma_{ijkl}(\mathbf{x}', \mathbf{x})\dot{\varepsilon}^p_{kl}(\mathbf{x})d\Omega(\mathbf{x}) + \frac{1}{2}f_{ij}(\dot{\varepsilon}^p_{kl})\right] \quad \text{(Eq 12)}$$

### 3.1 Incremental and Iterative Strategies

Nonlinear problems are usually solved by adopting a load incremental procedure and by iterating on a particular equation. If the unknowns (initial strains in this case) appear explicitly and are not known a priori, a recursive relationship among the stresses, the boundary unknowns, and the plastic strains must be used. Iterations are carried out until equilibrium, compatibility, and constitutive/plasticity relationships are all satisfied. The iterative scheme used here is described in Ref 23 and does not depend on the loading technique. The definition of the load increments and the loading path can, however, depend on whether the problem is load or displacement controlled. The type of problems analyzed here are load controlled, and the loading is monotonic, which simplifies the incremental strategy.

The stresses are calculated by assuming elastic behavior for a given initial load. The highest of the calculated stresses is made equal to the yield stress by scaling down or up accordingly. This defines the load at first yield. Subsequent load increments are found by adding to the previous one a percentage of the initial load. In crack problems, the highest stresses occur at the nodes of the discontinuous cells adjacent to the crack tip.

### 3.2 Crack Growth Analysis

Numerical simulation of crack propagation requires an incremental crack extension analysis; at each new position of the crack-tip, stress intensity factors are calculated in the new configuration. By using appropriate criteria it is possible to redefine the direction of the crack path at each increment.

Recently Leitao, Aliabadi, and Rooke (Ref 24) presented a formulation for elastoplastic crack growth analysis using BEM. This method is used here to simulate crack growth in the presence of residual stresses. Crack growth is simulated by allowing the crack to grow by a fixed amount (defined by the size of the elements on the crack faces) for a constant load applied at the extremes of the component; this load corresponds to the maximum value of the fatigue load. The minimum load was assumed to be zero. At each stage of the crack growth, nonlinear J-integrals (i.e., $T^*$ integrals) are obtained. The $T^*$ integral, defined by Atluri (Ref 25), is given as:

$$T^* = \lim_{\rho \to 0}\int_{\Gamma_\rho}(W_{n_1} - t_i u_{i,1})d\Gamma \quad \text{(Eq 13)}$$

where $W$ is the strain energy density and $\rho$ is the radius of a contour $\Gamma_\rho$ surrounding the crack tip. Applying Green's theorem to the above equation gives:

$$T^* = \int_{\Gamma'}(W_{n_1} - t_i u_{i,1})d\Gamma - \lim_{\rho \to 0}\int_{\Omega-\Omega_\rho}\left[W_1 - \frac{\partial}{\partial x_j}(\sigma_{ij}u_{i,1})\right]d\Omega \quad \text{(Eq 14)}$$

where $\Omega$ is the region within a general contour $\Gamma'$ and $\Omega_\rho$ is the region within $\Gamma_\rho$.

Equivalent stress intensity factors (i.e., $K_I^{max} = \sqrt{T^*E}$, $K_I^{min} = 0$) are then calculated, and the fatigue crack growth parameters $\Delta K$ and $R$ can now be determined for use in a crack growth prediction.

## 4. Prediction of Fatigue Crack Growth

### *4.1 Fatigue Crack Growth*

Crack growth can be induced by several mechanisms of which fatigue due to cyclic loading is the most important. It is a basic assumption of LEFM that the growth of a crack is controlled by the stress field surrounding the crack tip. As the stress intensity factor $K$ characterizes this stress field, it must also control the fatigue crack growth, which can be expressed as the distance, $da$, a crack of length $a$ moves per number of cycles, $dN$. Several models reported in the literature suggest that the rate of growth per cycle of stress ($da/dN$) is a function of the stress intensity factor range, $\Delta K = K_{max} - K_{min}$, the ratio, $R = K_{min}/K_{max}$, and of some material characteristics, here represented by $C$. The general empirical function can be expressed as:

$$\frac{da}{dN} = f(\Delta K, R, C) \qquad \text{(Eq 15)}$$

Instead of an empirical expression, a computer program that extrapolates and interpolates experimental data was used. This computer program (Ref 26) utilizes a database of $da/dN$ versus $\Delta K$ for various $R$ ratios for the BS2L65 aluminum alloy used in the experiments. For a given $R$ value and stress intensity factor range, the program interpolates between the specified data points or extrapolates outside them in order to obtain the crack growth rate (in practice a set of curves for alternating stress intensity factor against crack rate, each curve being at a constant value of the ratio $R$).

### *4.2 Numerical Application (LEFM/WF)*

The effect on fatigue crack growth of the application of a life enhancement technique known as prestressing is reported in this section. The prestressing, or overloading, involves subjecting the specimen to a single load large enough to produce local plasticity in the vicinity of the hole thus creating a residual stress field on unloading. This is very simple to perform under experimental conditions, but its usage is restricted to laboratory studies.

**Uncracked Components.** The specimen geometry and material properties are as shown in Fig. 1. Plane stress conditions are assumed. The specimen has initially undergone prestressing. The prestressing technique involved applying an increasing load to the ends of the specimen until the material undergoes plastic deformation around the stress concentration at the edge of the circular hole, and then removing the load. This technique was used by Cook et al. (Ref 19) in their experimental study of the specimen shown in Fig. 1. The specimen universal number is 2014 with heat treatment T6 and rolling direction LT. See ESDU (Engineering Services Data Unit) data sheet L 168. The specimens tested were subjected to uniaxial fatigue loading; the loading was constant amplitude sinusoidal with a mean stress of 110 $Nmm^{-2}$ on the net section. The amplitude corresponds to minimum and maximum gross section stresses of 3.03 $Nmm^{-2}$ and 46.34 $Nmm^{-2}$ at the free end.

Prestressing was modeled numerically by the application of a single uniaxial tensile load at both ends of the specimen. This load caused local plasticity in the region around the central hole. On removal of this load, a residual stress field remained. Three overloads were used, namely 237, 277, and 317 *KN*, which resulted in average net stresses equivalent to 60%, 70%, and 80% of the 0.1% proof stress (i.e., $\sigma_Y$ = 465 $Nmm^{-2}$).

For the numerical analysis two different models must be considered. An elastoplastic model is used to obtain the residual stress field due to the prestress, for which a BEM elastoplastic analysis is carried out. The residual stress distribution across the test section induced by the prestress technique is shown in Fig. 2. In all cases, the residual stress distribution was compressive at the edge of the hole, becoming tensile further away before tending to zero. A linear elastic model is used to obtain the stress intensity factors due to the total load. These stress intensity factors were evaluated over the range of crack lengths judged relevant. The following crack lengths were considered: 0.4, 0.65, 1.0, 1.35, 2.0, 3.0, 4.0, and 5.0 mm.

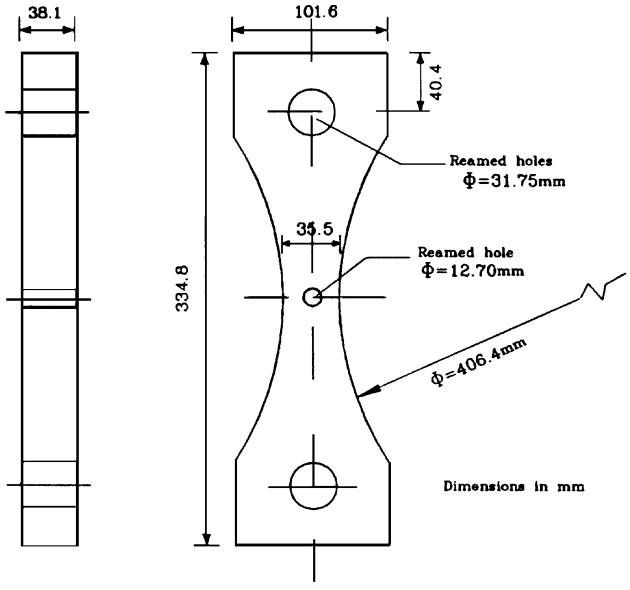


**Fig. 1** Fatigue test specimen

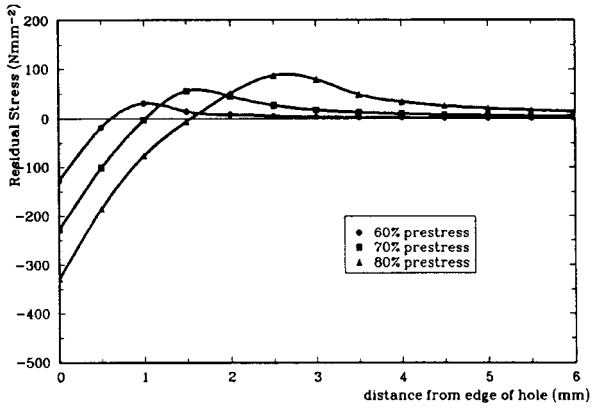


**Fig. 2** Residual stress distributions due to the prestress

The variation of $K_{res}$ with crack length for each prestress value is shown in Fig. 3. $K_{res} = 0$ for the uncracked body and reaches its maximum negative value at the highest prestress level for a crack length of approximately 0.8 mm. $K_{res}$ then increases to a small positive value at longer crack lengths. Figure 4 shows the variation of $K_{tot}$ with crack length for the various prestress levels. The reductions in $K_{tot}$ with increasing prestress, at short crack lengths, follow directly from the increases in compressive residual stress fields.

**Initially Cracked Specimens.** Cracked components are normally repaired by removing the damage and possibly using a life enhancement treatment such as cold expansion. It may not always be practical to remove some or all of the damage, and even after the removal treatment, there remains the possibility that some damage will remain. Simulation of this type of structural repair is achieved by modeling the prestressing of an initially cracked specimen.

As for the previous section, the numerical analysis requires two different models. First is an elastoplastic model similar to the one described, except for the fact that now the analysis is repeated for the range of initial cracks adopted; these are 1, 2, and 3 mm. Semidiscontinuous boundary elements and cells are used in the area adjacent to the crack tip to avoid difficulties with the modeling of the singularity of the tractions and stresses at that point. The same prestress levels as in the previous example were used. Second, the same linear elastic model as that for the uncracked component above was used.

The residual stress variation with position, ahead of the crack, is shown in Fig. 5 at each overload level for the three initial cracks. In Fig. 6, the same stress fields are represented for the three overload levels at each initial crack, except for the largest, where only the first two overload levels are shown. Plastic collapse was attained for the highest overload at the largest initial crack. Crack growth predictions from the initial crack length as a function of the number of cycles are represented in Fig. 7.

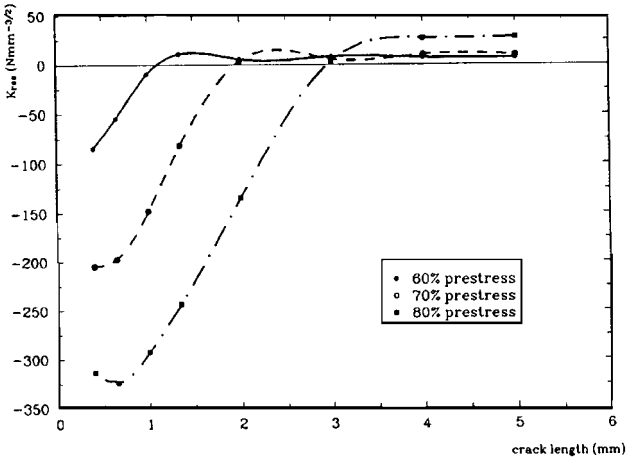


**Fig. 3** Stress intensity factor, *K*, due to residual stresses

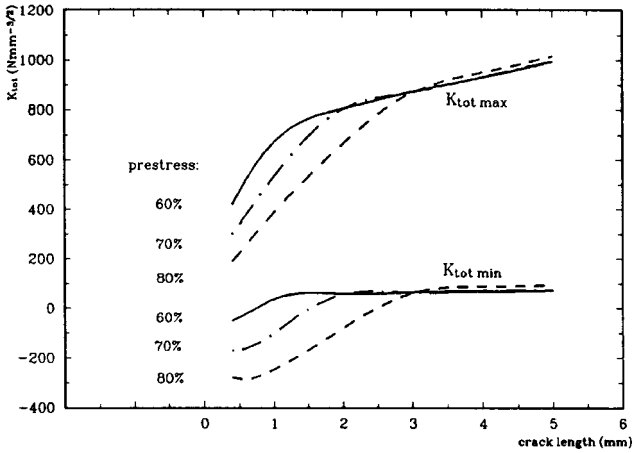


**Fig. 4** Stress intensity factor, *K*, due to applied and residual stresses

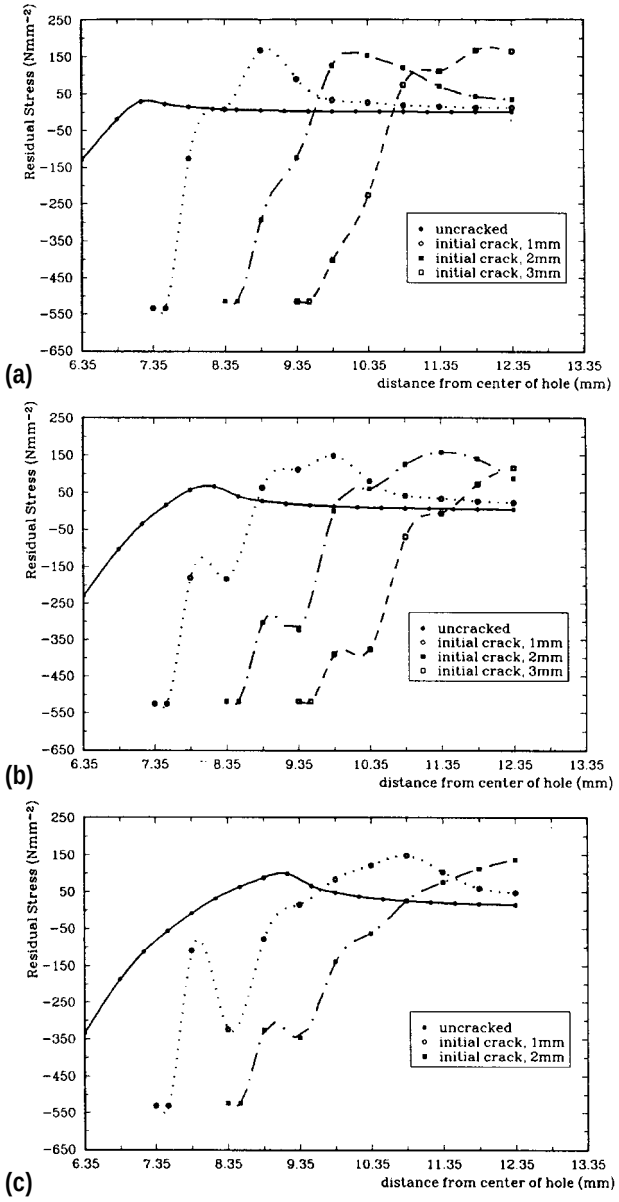


**Fig. 5** Residual stress distributions (a) 60% prestress, (b) 70% prestress, and (c) 80% prestress

Comparison of Fig. 3 and 5 shows that the residual stresses are more compressive for the precracked than for the uncracked components. The distribution of these stresses ahead of the initial crack is similar for all crack lengths at each overload. The depth of plastically deformed material increases with increasing magnitude of overload at each initial crack length. Fatigue lives reflect the effect of these residual stresses. The number of cycles to failure increases appreciably with the level of prestress applied and the initial crack length. Figure 7 shows that the ratio of life after prestress of cracked specimens over the residual life of uncracked specimens increases with initial crack length.

### *4.3 Numerical Application (EPFM/J)*

In this section, the crack growth procedure based on elastoplastic fracture mechanics and a nonlinear J-integral, as described in the earlier section, is applied to the specimen. The specimen is subjected to the same prestress levels with initial crack sizes of 0.5, 1.0, and 2.0 mm.

The stress intensity factors, calculated from the $T^*$ integral, were evaluated over the range of crack lengths judged relevant. The following crack lengths were considered: 0.5, 1.0, 2.0, 3.0, 4.0, and 5.0 mm. The load applied to the ends of the specimen corresponded to a gross section stress of 46.34 $Mmm^{-2}$.

**Crack Growth of Initially Uncracked Specimens.** Parameters such as COD and CTOD give indications about the fracture process. Even if these parameters are not used to predict crack growth, it is interesting to have an idea of the displacements of the crack faces (crack profiles) at a certain crack extension stage. Figure 8 shows the crack surface profiles as predicted during the crack growth simulation of all the cases analyzed, namely the three prestress loads and the nontreated

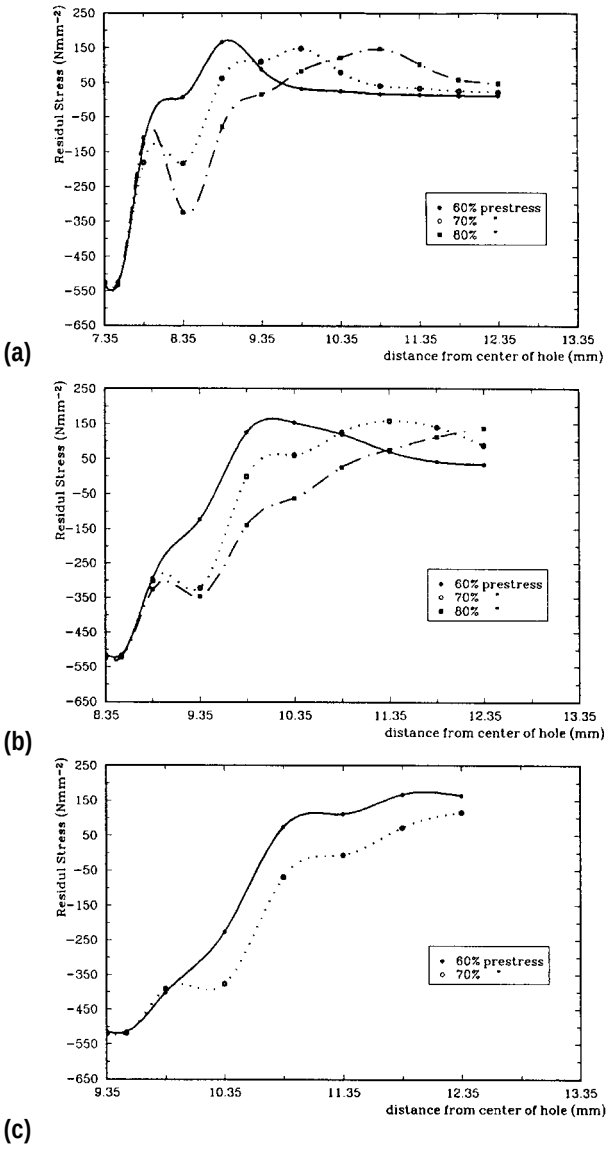


**Fig. 6** Residual stress distributions (a) 1 mm initial crack, (b) 2 mm initial crack, and (c) 3 mm initial crack

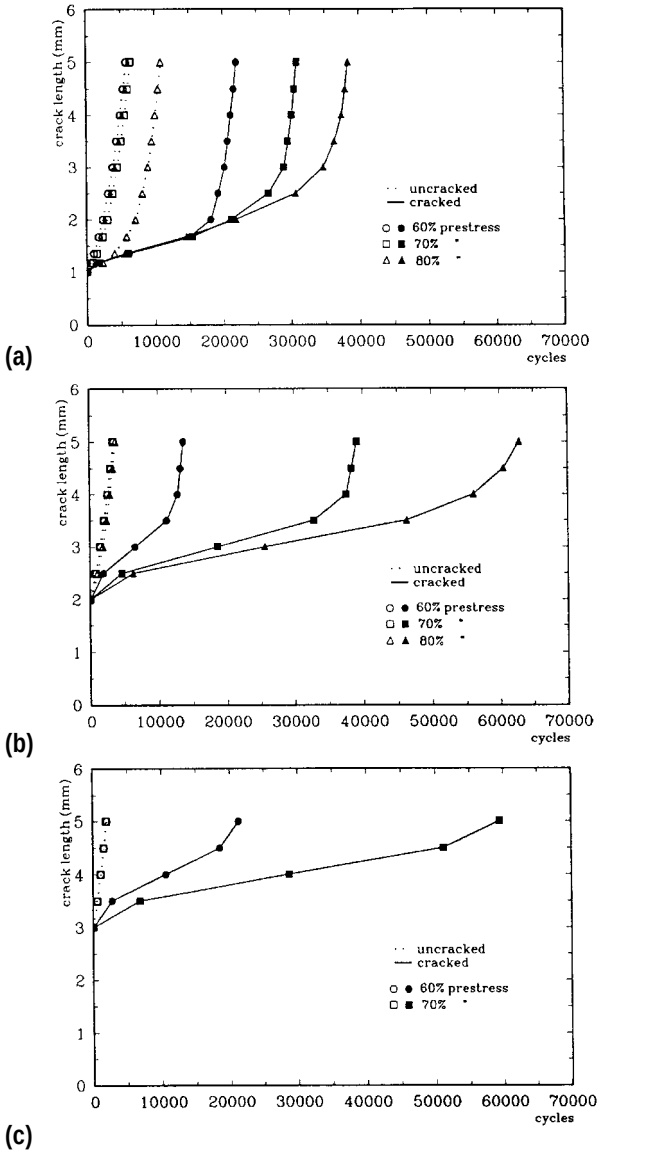


**Fig. 7** Variation of crack length with the number of cycles (a) 1 mm initial crack, (b) 2 mm initial crack, and (c) 3 mm initial crack

case. The crack surface profiles from earlier elastic crack propagation analysis are also represented in the same figure.

The roughness of the profiles, especially for longer cracks, is partly due to the use of discontinuous boundary elements on the crack faces but, above all, to the element release technique developed. Smoother profiles can be obtained if more elements are used in the crack region. Because the differences are not significant, the refinement of the boundary mesh was not considered necessary.

The component of the displacement normal to the crack decreases for increasing prestress level. This decrease is relatively more important for shorter cracks than for longer cracks. This is expected since the region of compressive residual stresses increases with the prestress level and because the magnitude of these stresses are greater close to the edge of the hole. Close to the crack tip and for all the situations, the profiles are very similar after the first two or three crack extensions. This is probably because the cracks have grown beyond the initial plastic region (approximately 2 mm for the highest prestress level). At the edge of the hole, in the crack mouth region, there is a tendency for the crack faces to become flat especially for longer cracks at the highest prestress level.

The angle the crack faces makes at the crack tip, CTOA, is another important crack growth criterion. Without attempting to quantify this parameter, it seems that it stabilizes after the third crack extension. This may be related to the fact that the crack extends by constant amounts: 0.5 mm for the first two extensions and 1 mm for the subsequent ones. The same can be said for the COD. These two parameters, although widely used, are problematic because it is difficult to define where exactly any measurements should be made.

**Crack Growth Rates.** Predicted crack growth for the three prestress values are shown in Fig. 9(a-c) together with experimental data (Ref 19). In these figures, the computed values include both the LEFM/WF model and the EPFM/J model. The comparison of the predictions shows good agreement with experimental results for the range of cracks analyzed. The difference between the two sets of predictions seems to be more important for higher prestress levels and in the region of shorter cracks. This suggests that further research should concentrate on the region of short cracks.

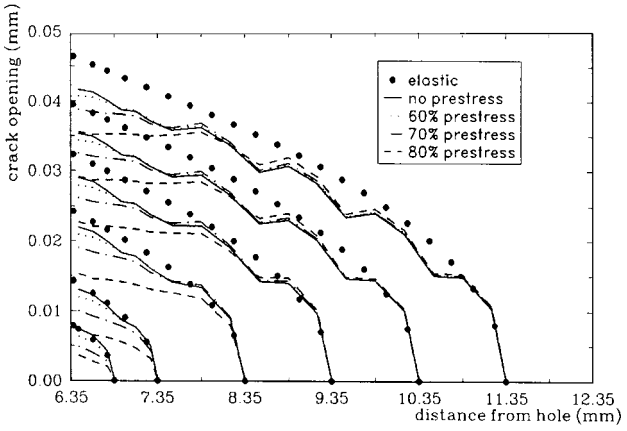


**Fig. 8** Crack surface profiles

**Crack Growth of Initially Cracked Specimens.** The case of precracked specimens being subjected to prestressing is analyzed here. The simulation of the growth of cracks in the presence of the residual stresses created by prestressing is carried

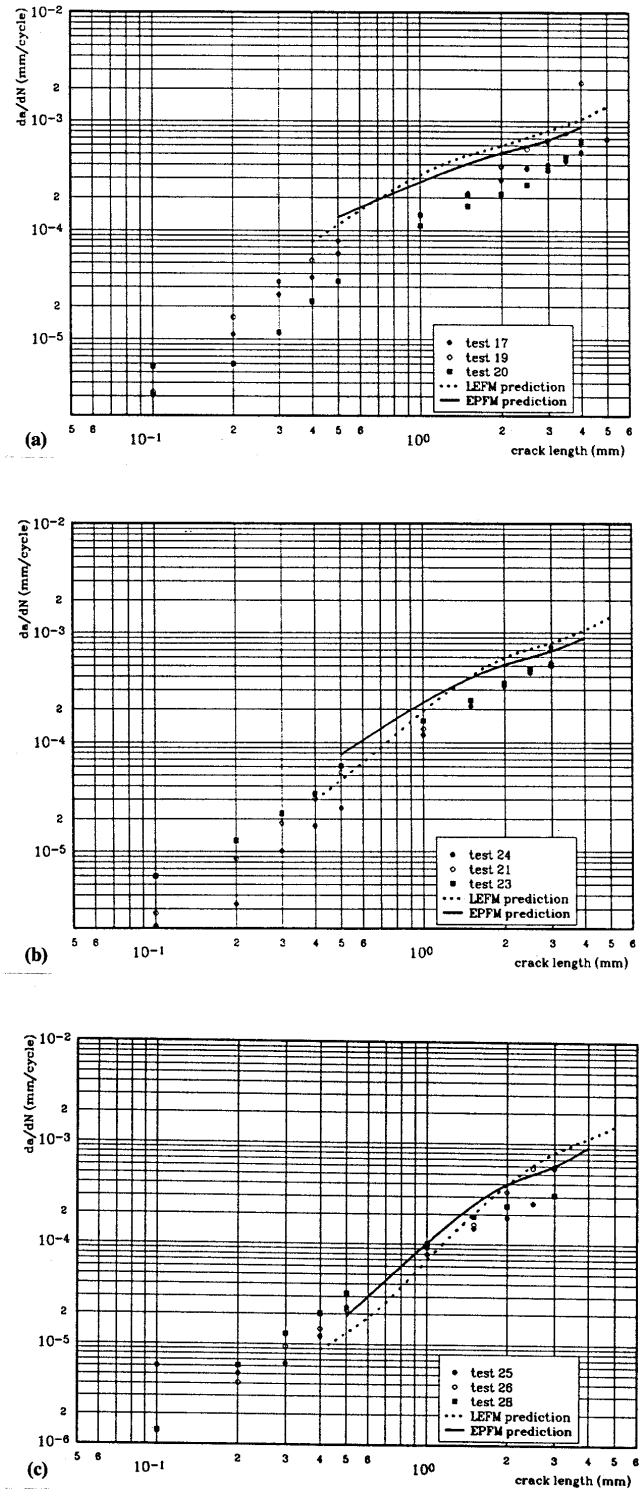


**Fig. 9** Comparison of predicted and experimental crack growth rates for (a) 60% prestress, (b) 70% prestress, and (c) 80% prestress

out in a similar way to that of initially uncracked specimens. The only difference is the presence of the initial crack.

The crack surface profiles for the crack growth simulation of precracked specimens are shown in Fig. 10. The effect of prestressing initially cracked specimens is characterized, in all the cases, by two main aspects. First, there is an abrupt change in the profile of crack opening at the position of the original crack tip. Second, in the region that goes from the crack mouth to the initial crack tip, the normal displacements are much closer to the elastic crack profiles especially for the longer cracks.

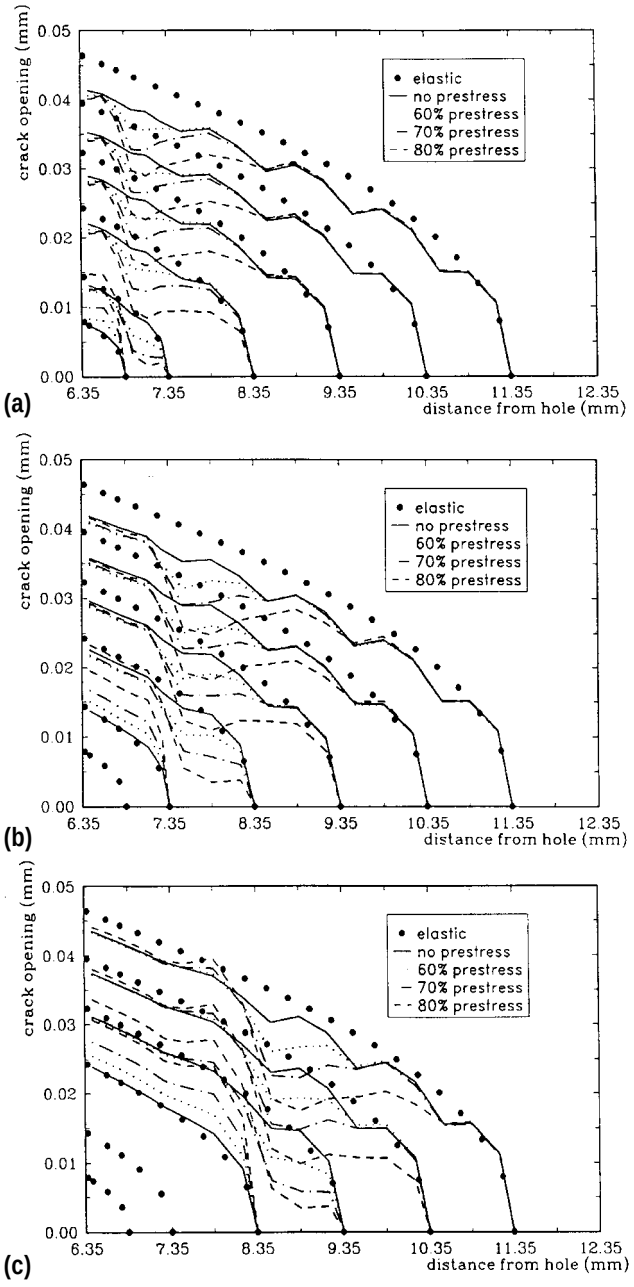


**Fig. 10** Crack surface profiles for (a) initial crack of 0.5 mm, (b) initial crack of 1.0 mm, and (c) initial crack of 2.0 mm

## 5. Conclusions

Fatigue crack growth through a residual stress field due to prestressing was analyzed using the usual LEFM approach as well as a new nonlinear EPFM approach. The results were in reasonable agreement to each other as well as experimental measurements. The EPFM approach appears to be superior to the LEFM approach for the highest prestress level and the shortest cracks, where plastic deformation is likely to be most significant. In addition, the application of the life enhancement techniques can only be studied in detail with the EPFM technique.


### Acknowledgment

This work has been carried out with the support of the Ministry of Defence, Defence Evaluation and Research Agency, Farnborough, Hants., U.K.


### References


1. R.M. Potter and A.F. Grandt, An Analysis of Residual Stresses and Displacements due to Radial Expansion of Fastener Holes, *ASME Failure Prevention and Reliability Conference* (Washington, D.C.), MacDonald-Boeing, Long Island, NY, 1975
2. D.L. Rich and I.F. Impellizzeri, Fatigue Analysis of Cold-Worked and Interface Fit Fastener Holes, *Report McDonnell Aircraft Company Mcair,* 76-007, 1976
3. J.B. Chang, Prediction of Fatigue Crack Growth at Cold-Worked Fastener Holes, *J. Aircraft,* Vol 14, 1977, p 903-908
4. T.M. Hsu and J.A. Aberson, Analysis and Correlation of Crack Growth from Cold-Worked Fastener Holes, *Advanced Structures Department,* Lockheed-Georgia Company, 1966, p 40-47
5. J.L. Rudd, T.M. Hsu, and J.A. Aberson, Analysis and Correlation of Crack Growth from Interference-Fit Fastener Holes, *Proc. of the First International Conf. on Numerical Methods in Fracture Mechanics,* A.R. Luxmoore and D.R.J. Owen, Ed., 1978, p 774-786
6. H. Armen, A. Levy, and H.L. Eidinoff, Elastic-Plastic Behaviour of Cold-Worked Holes, *J. Aircraft,* Vol 21, 1984, p 193-201
7. R. Cook, D.P. Rooke, A. Smith, and A. Bowles, Residual Stress Fields at Notches: Effect on Fatigue Crack Growth, *Technical Report 85049,* Royal Aircraft Establishment, 1985
8. J.Y. Mann and J.G. Sparrow, Cold Expansion to Extend the Fatigue Lives of Structures, *Proc. of the 10th Australian Conf. on the Mechanics of Structures and Materials,* Adelaide, 1986, p 93-99
9. O. Buxbaum and H. Huth, Expansion of Cracked Fastener Holes as a Measure for Extension of Lifetime to Repair, *Eng. Fract. Mechanics,* Vol 28, 1987, p 689-698
10. M. Heller, R. Jones, and J. Williams, Analysis of Cold-Expansion for Cracked and Uncracked Fastener Holes, *Eng. Fract. Mechanics,* Vol 39, 1991, p 195-212
11. M. Heller and R. Carey, Stress Analysis of Interface-Fit Fastener Holes Using a Penalty Finite Element Method, *Computers and Structures,* Vol 41, 1991, p 73-81
12. G. Clarck, Modelling Residual Stress and Fatigue Crack Growth at Cold-Expanded Fastener Holes, *Fatigue Frac. Eng. Mater. Struct.,*Vol 14, 1991, p 579-589
13. *Computer Methods and Experimental Measurements for Surface Treatment Effects,*, M.H. Aliabadi and C.A. Brebbia, Ed., Computational Mechanics Publications, 1993
14. M.H. Aliabadi and A. Terranova, *Computer Methods and Experimental Measurements for Surface Treatment Effects II,* Computational Mechanics Publications, 1995

15. V. Leitao, M.H. Aliabadi, R. Cook, and D.P. Rooke, Boundary Element Analysis of Fatigue Crack Growth in the Presence of Residual Stresses, in *Proc. of the Second Int. Conf. on Computer Aided Assessment and Control of Localized Damage*, Computational Mechanics Publications, Southhampton, UK, 1992, p 489-510
16. V.M.A. Leitao, M.H. Aliabadi, and D.P. Rooke, The Dual Boundary Element Formulation for Elastoplastic Fracture Mechanics, *Int. J. Num. Meth. Eng.*, Vol 38, 1995, p 315-333
17. M.H. Aliabadi and D.P. Rooke, *Numerical Fracture Mechanics*, Kluwer Academic Publishers, Dordrecht and Computational Mechanics Publications, 1991
18. H.F. Bueckner, Field Singularities and Related Representations, *Methods of Analysis and Solutions of Crack Problems, Mechanics of Fracture I*, G.C. Sih, Ed., Noordhoff, Leyden, 1973, p 239-314
19. R. Cook, D.P. Rooke, A. Smith, and R. Bowles, "Residual Stress Fields at Notches: Effect on Fatigue Crack Growth," RAE Technical Report 85049, Royal Aircraft Establishment, Farnborough, 1985
20. M.H. Aliabadi, D.P. Rooke, and D.J. Cartwright, Fracture Mechanics Weight Functions by the Removal of Singular Fields using Boundary Element Analysis, *Int. J. Fracture*, Vol 40, 1989, p 271-284
21. V.M.A. Leitao, M.H. Aliabadi, and D.P. Rooke, Advanced Boundary Elements for Nonlinear Fracture Mechanics, *Adv. Computational Methods in Structural Mechanics*, M. Papadrakakis and G. Bugenda, Ed., CIMNE, Barcelona, 1996, p 166-184
22. A. Mendelson, "Boundary Integral Methods in Elasticity and Plasticity," Report No. NASA TN D-7418, NASA, 1973
23. V.M.A. Leitao, Boundary Elements in Nonlinear Fracture Mechanics, *Topics in Engineering*, Vol 21, Computational Mechanics Publications, 1994
24. V.M.A. Leitao, M.H. Aliabadi, and D.P. Rooke, Elastoplastic Simulation of Fatigue Crack Growth: Dual Boundary Element Formulation, *Int. J. Fatigue*, Vol 17, 1995, p 353-363
25. S.N. Atluri, Energetic Approaches and Path-Independent Integrals in Fracture Mechanics, *Computational Methods in the Mechanics of Fracture*, S.N. Atluri, Ed., North-Holland, 1986, p 121-162
26. P.R. Edwards, A Computer Program for the Interpolation and Extrapolation of Crack Propagation Data, CP-1387 Structures Dept., Royal Aircraft Establishment, Farnborough, U.K., 1977